19th International Conference
ENGINEERING MECHANICS 2013
Svratka, Czech Republic, May 13 – 16, 2013

Identification of Parameters of the Feigenbaum-Dafalias Directional Distortional Hardening Model

S. Parma, J. Plešek, Z. Hrubý, R. Marek,[1] H. P. Feigenbaum[2], Y. F. Dafalias[3,4]

Summary: *Distortion of yield surface was observed in numerous experiments with various types of metals. The distorted surface shows high curvature in the direction of load and flattening in the opposite direction. Feigenbaum and Dafalias (2008) proposed a new phenomenological model to capture this phenomenon. In sum, Feigenbaum-Dafalias directional distortional model includes six independent material parameters to be identified. The present paper describes an identification algorithm for parameters of the model.*

Keywords: ***plasticity, directional distortional hardening, identification***

1. Introduction

Modern experiments show distortion of yield surface due to strain hardening, see e.g. Wu & Yeh (1991). The distorted yield surface becomes highly curved in the load direction, while in the opposite direction, it becomes flatter. In order to describe this phenomenon, several models were developed, see e.g. Ortiz and Popov (1983) and Francois (2001).

Feigenbaum and Dafalias (2007) presented a model involving the fourth-order tensor to capture the effect of distortion. Evolution equations of internal variables of the model are derived to meet the dissipation inequality. Further, Plešek (2010) discussed sufficient conditions to maintain convexity of distorted yield surface. This convexity guarantees convergence of return mapping numerical integrators, as shown in Plešek (1997).

Later, Feigenbaum and Dafalias (2008) presented a simplified form of the model, where the fourth-order tensor is reduced to the dot product of inner variables multiplied by one distortional parameter c only. The model is referred to as the α-model with constant distortional parameter and includes six parameters in total.

In this paper, the identification algorithm for model's parameters is proposed and verified on virtual experimental data. The algorithm is based on two categories of experimental data. The

[1] Ing. Slavomír Parma, Ing. Jiří Plešek, CSc., Ing. Zbyněk Hrubý, Ph.D., Ing. René Marek, Institute of Thermomechanics AS CR, v. v. i., Dolejškova 1402/5, 182 00 Prague 8, Czech Republic, e-mail plesek@it.cas.cz, parma@it.cas.cz, zbynek@it.cas.cz, marek@it.cas.cz
[2] Department of Mechanical Engineering, Northern Arizona University, PO Box 15600, Flagstaff, AZ 86011, USA, e-mail heidi.feigenbaum@nau.edu
[3] Department of Civil and Environmental Engineering, University of California at Davis, Davis, CA 95616, USA, e-mail jfdafalias@ucdavis.edu
[4] Department of Mechanics, Faculty of Applied Mathematical and Physical Science, National Technical University of Athens, Zographou, 15780, Greece, e-mail yfdafalias@central.ntua.gr

first ones are the stress-strain curves with unloading at certain strain levels. The second one is the yield surface distorted at certain level of developed plastic strain.

The text is organized as follows. Section 2 overviews the α-model with fixed distortional parameter. In Section 3, analytical relations for fundamental load cases are provided. In Section 4, relations from Section 3 section are compared with experimental data. The comparison yield to system of ten nonlinear equations for six unknown parameters which is solved in a closed-form.

In Section 5, identification algorithm is verified. Since no complex experimental data are available, virtual ones are used instead. Finally, identification algorithm is evaluated.

2. Feigenbaum-Dafalias Simple Directional Distortional Hardening Model

Feigenbaum and Dafalias (2008) proposed simplified form of their general directional distortional hardening model. In this simplified form, the yield function is given by

$$f(\boldsymbol{\sigma}) = \frac{3}{2}\left[1 - c\left(\boldsymbol{n}_{\mathrm{r}} : \boldsymbol{\alpha}\right)\right](\boldsymbol{s} - \boldsymbol{\alpha}) : (\boldsymbol{s} - \boldsymbol{\alpha}) - k^2 = 0. \tag{1}$$

Here, $\boldsymbol{\sigma}$ is the stress tensor; $\boldsymbol{s}$ is the deviatoric stress tensor; $\boldsymbol{\alpha}$ is the backstress tensor; c is a positive material parameter; k is a scalar internal variable; the double dot symbol represents the inner product of two tensors as in $\boldsymbol{\alpha} : \boldsymbol{\beta} = \alpha_{ij}\beta_{ij}$. Finally,

$$\boldsymbol{n}_{\mathrm{r}} = \frac{\boldsymbol{s} - \boldsymbol{\alpha}}{\|\boldsymbol{s} - \boldsymbol{\alpha}\|} \tag{2}$$

is the unit tensor pointing in the direction of load relatively to the center of the yield surface, and $\|.\|$ denotes the Euclidean norm of a second order tensor.

The model's internal variables are governed by the standard evolution equations. Plastic strain obeys the associated flow rule

$$\dot{\boldsymbol{\epsilon}}^{\mathrm{p}} = \lambda \frac{\partial f}{\partial \boldsymbol{\sigma}}, \tag{3}$$

the kinematic hardening rule of Armstrong-Frederick's type retains the evanescent memory member so that

$$\dot{\boldsymbol{\alpha}} = a_1 \left(\dot{\boldsymbol{\epsilon}}^{\mathrm{p}} - a_2 \|\dot{\boldsymbol{\epsilon}}^{\mathrm{p}}\| \boldsymbol{\alpha}\right), \tag{4}$$

and similarly for the isotropic part

$$\dot{k} = \lambda \kappa_1 k \left(1 - \kappa_2 k\right). \tag{5}$$

The initial values at time $t = 0$ are defined as $\dot{\boldsymbol{\epsilon}}^{\mathrm{p}} = \boldsymbol{0}$, $\boldsymbol{\alpha} = \boldsymbol{0}$ and $k = k_0$, that is, k_0 is the initial yield stress. Details of this constitutive model are presented in Feigenbaum and Dafalias (2008).

For further, it is useful to have some formulas ready. One may explicitly express the gradient

$$\frac{\partial f}{\partial \boldsymbol{\sigma}} = \frac{3}{2}\|\boldsymbol{s} - \boldsymbol{\alpha}\| \left[2\boldsymbol{n}_{\mathrm{r}} - c\left(\boldsymbol{n}_{\mathrm{r}} : \boldsymbol{\alpha}\right)\boldsymbol{n}_{\mathrm{r}} - c\boldsymbol{\alpha}\right] \tag{6}$$

and its norm as

$$\left\| \frac{\partial f}{\partial \boldsymbol{\sigma}} \right\| = \frac{3}{2}\|\boldsymbol{s} - \boldsymbol{\alpha}\| \sqrt{\left[2 - c\left(\boldsymbol{n}_{\mathrm{r}} : \boldsymbol{\alpha}\right)\right]\left[2 - 3c\left(\boldsymbol{n}_{\mathrm{r}} : \boldsymbol{\alpha}\right)\right] + c^2 \boldsymbol{\alpha} : \boldsymbol{\alpha}}. \tag{7}$$

Moreover, the gradient yield

$$\frac{\partial f}{\partial \boldsymbol{\sigma}} = \left\| \frac{\partial f}{\partial \boldsymbol{\sigma}} \right\| \boldsymbol{n}, \tag{8}$$

where $\boldsymbol{n}$ is the outward unit normal to the yield surface.

It was proved in Feigenbaum and Dafalias (2008) and Plešek (2010) that the necessary and sufficient condition, which renders dissipation positive and, simultaneously, preserves strict convexity for all times, reads

$$\|c\boldsymbol{\alpha}\| < 1. \tag{9}$$

For monotonic loading and as $t \to +\infty$, the saturated state is reached when

$$\boldsymbol{n} - a_2 \boldsymbol{\alpha} = \boldsymbol{0}. \tag{10}$$

Since $\boldsymbol{\alpha}$ starts from zero and the magnitude of the limit backstress is $1/a_2$, one may write

$$\|\boldsymbol{\alpha}\| \leq 1/a_2. \tag{11}$$

Equation (10) and Inequality (11) yield

$$c < a_2. \tag{12}$$

This constraint needs to be satisfied anytime.

To illustrate behavior of the discussed model, simulations of distortion of the yield surface are plotted. Figure 1 shows the evolution of subsequent yield surfaces in two subspaces. Here, material is loaded by uniaxial tension until the limit state has been reached. Material parameters are taken from Feigenbaum (2008). Thus, $a_1 = 10\,500\,\mathrm{MPa}$, $a_2 = 0.02\,\mathrm{MPa}^{-1}$, $\kappa_1 = 6\,000\,\mathrm{MPa}$, $\kappa_2 = 0.012\,\mathrm{MPa}^{-1}$, $c = 0.019\,\mathrm{MPa}^{-1}$, $k_0 = 128\,\mathrm{MPa}$. Note, that the condition stipulated by Inequality (12) is fulfilled.

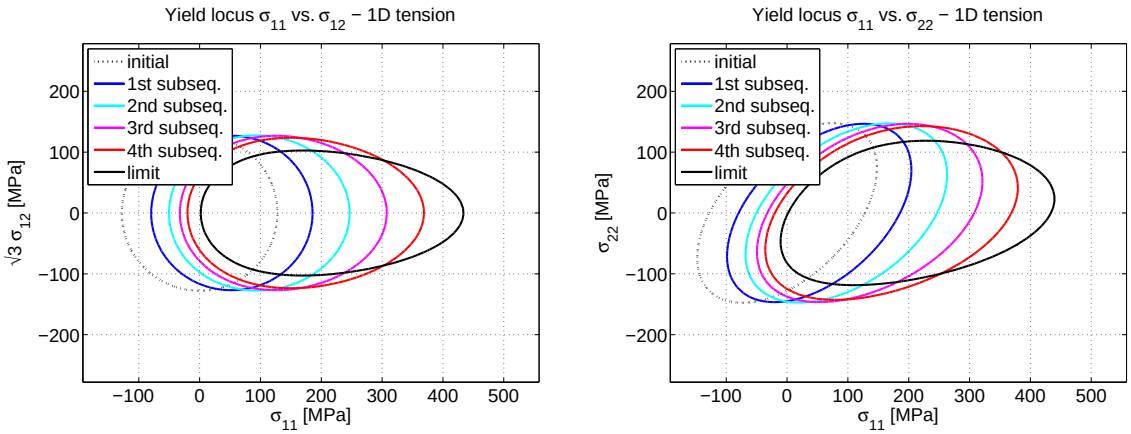

Figure 1: The gradual distortion of the yield surface due to uniaxial tension shown in the two sub-spaces.

3. Analytical Relations for Fundamental Loading Cases

In this section, analytical models of the stress-strain curve for tensile/compression loading (SSC) and the distorted yield surface (DYS) in the σ–$\sqrt{3}\tau$ space are derived.

In case of uniaxial tension, Equations (3), (4), and (5) lead to relations for isotropic and kinematic part of hardening

$$\dot{\alpha}_{11} = a_1 \dot{\epsilon}^{\mathrm{p}}_{11} \left(1 - a_2 \sqrt{\frac{3}{2}}\, \alpha_{11}\, \mathrm{sgn}\, (s_{11} - \alpha_{11}) \right), \tag{13}$$

$$\dot{k} = \kappa_1 (1 - \kappa_2 k) \frac{\dot{\epsilon}^{\mathrm{p}}_{11}\, \mathrm{sgn}\, (s_{11} - \alpha_{11})}{\sqrt{1 - c \sqrt{\frac{3}{2}}\, \mathrm{sgn}\, (s_{11} - \alpha_{11})\, \alpha_{11}}}. \tag{14}$$

Henceforth, the term ' sgn $(s_{11} - \alpha_{11})$' will be denoted as sgn .

Using

$$\frac{\mathrm{d}g}{\mathrm{d}t} = \frac{\mathrm{d}g}{\mathrm{d}\epsilon^{\mathrm{p}}_{11}} \frac{\mathrm{d}\epsilon^{\mathrm{p}}_{11}}{\mathrm{d}t}, \tag{15}$$

Equations (13) and (14) yield the final form

$$\alpha'_{11} = a_1 \left(1 - \sqrt{\frac{3}{2}}\, a_2 \alpha_{11}\, \mathrm{sgn} \right), \tag{16}$$

$$k' = \frac{1}{2} \frac{\kappa_1 (1 - \kappa_2 k)\ \mathrm{sgn}}{\sqrt{1 - \sqrt{\frac{3}{2}}\, c\, \alpha_{11}\, \mathrm{sgn}}}, \tag{17}$$

where $(.)'$ operator is defined as $(.)' \equiv \frac{\mathrm{d}(.)}{\mathrm{d}\epsilon^{\mathrm{p}}_{11}}$.

Integrating Equation (16), one obtains closed-form solution

$$\alpha_{11} = \sqrt{\frac{2}{3}}\, \frac{1}{a_2\, \mathrm{sgn}} \left[1 - \left(1 - \sqrt{\frac{3}{2}} a_2 \alpha_{11,0}\, \mathrm{sgn} \right) \cdot \exp \left(- \sqrt{\frac{3}{2}} a_1 a_2 \left(\epsilon^{\mathrm{p}}_{11} - \epsilon^{\mathrm{p}}_{11,0} \right)\ \mathrm{sgn} \right) \right], \tag{18}$$

where $\alpha_{11,0} = \alpha_{11} \left(\epsilon^{\mathrm{p}}_{11,0} \right)$ defines the initial condition. Solving of Equation (17) leads to the integral

$$\int \frac{\mathrm{sgn} \cdot \mathrm{d}\epsilon^{\mathrm{p}}_{11}}{\sqrt{1 - \sqrt{\frac{3}{2}}\, c\, \alpha_{11}\, \mathrm{sgn}}}, \tag{19}$$

where α_{11} is given by Equation (18). Assuming Inequality (12), and using substitutions $\sqrt{\frac{3}{2}}\, c\, \alpha_{11}\, \mathrm{sgn} = \varphi$, $\sqrt{1 - \varphi} = p$ and $\sqrt{\frac{a_2}{a_2 - c}}\, p = q$, it is possible to find the solution in

form

$$k = \frac{1}{\kappa_2}\Big[1 - (1 - \kappa_2 k_0) \cdot \exp \xi\Big], \tag{20}$$

$$\xi = -\sqrt{\frac{2}{3}}\,\frac{\kappa_1\kappa_2}{a_1\sqrt{a_2\,(a_2 - c)}}\Big(\tanh^{-1}(p) - \tanh^{-1}(p_0)\Big),$$

$$p(\epsilon^{\mathrm{p}}_{11}) = \sqrt{1 + \frac{c}{a_2 - c}\left(1 - \sqrt{\frac{3}{2}}\,a_2\alpha_{11,0}\,\mathrm{sgn}\right)\exp\left(-\sqrt{\frac{3}{2}}a_1a_2(\epsilon^{\mathrm{p}}_{11} - \epsilon^{\mathrm{p}}_{11,0})\,\mathrm{sgn}\right)},$$

$$p_0 = p(\epsilon^{\mathrm{p}}_{11,0}) = \sqrt{1 + \frac{c}{a_2 - c}\left(1 - \sqrt{\frac{3}{2}}\,a_2\alpha_{11,0}\,\mathrm{sgn}\right)}.$$

Thus, Equations (18) and (20) express the evolution of α_{11} and k, respectively. Finally, the stress tensor component σ_{11} can be expressed from Equation (1) by

$$\sigma_{11} = \mathrm{sgn} \cdot \frac{k}{\sqrt{1 - \sqrt{\frac{3}{2}}\,c\,\alpha_{11}\,\mathrm{sgn}}} + \frac{3}{2}\,\alpha_{11}. \tag{21}$$

Substituting Equations (18) and (20) into Equation (21), one obtains relation between the stress and strain in case of uniaxial load. Formally, Equation (21) may be rewritten as $\sigma_{11} = \sigma_{11}(\epsilon^{\mathrm{p}}_{11})$. The stress-strain curve is a special case of Equation (21), where $\mathrm{sgn} = 1$, $\epsilon^{\mathrm{p}}_{11,0} = 0$, $\alpha_{11,0} = \alpha_{11}\left(\epsilon^{\mathrm{p}}_{11,0}\right) = 0$ and $k\left(\epsilon^{\mathrm{p}}_{11,0}\right) = k_0$.

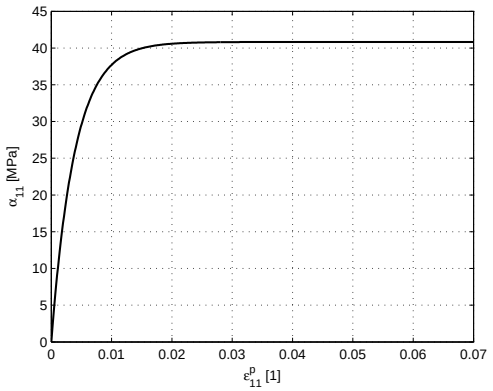

Figure 2: Relation $\alpha_{11} = \alpha_{11}(\epsilon^{\mathrm{p}}_{11})$

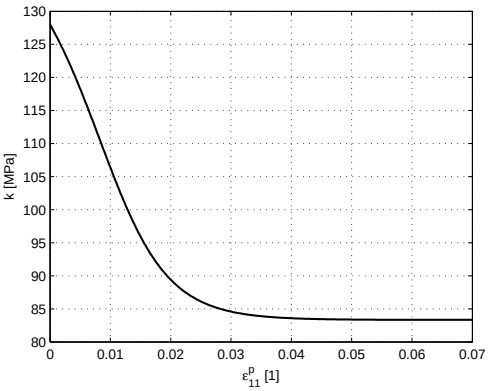

Figure 3: Relation $k = k(\epsilon^{\mathrm{p}}_{11})$

Regarding an analytical approximation of the distorted yield surface in the σ–$\sqrt{3}\tau$ space, suppose that uniaxial loading of material, which leads to the plastic deformation, is modeled. This load causes the distortion of the yield surface represented by the evolution of internal variables, the backstress component α_{11} and the k quantity. At a certain state, the loading is stopped, and material is unloaded, and subsequently, material is loaded by tension and shear (torsion) simultaneously.

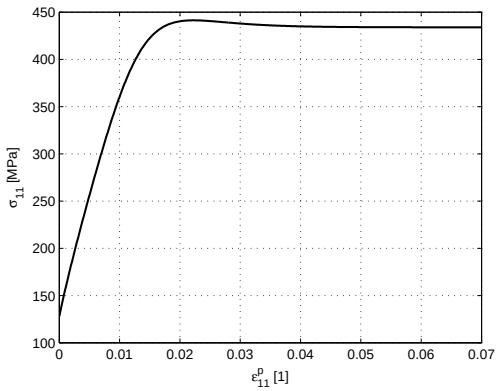

Figure 4: Relation $\sigma_{11} = \sigma_{11}(\epsilon^{\mathrm{p}}_{11})$

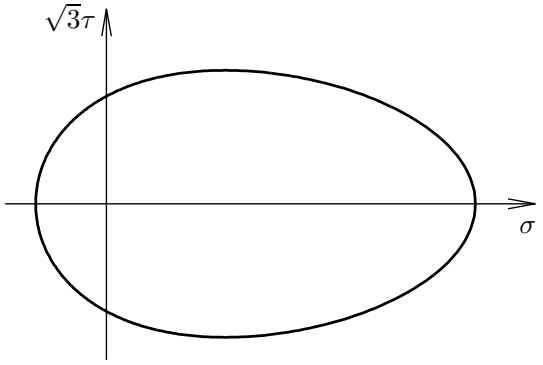

Figure 5: Distorted YS, relation $f\left(\sigma, \sqrt{3}\tau\right) = 0$

In σ–$\sqrt{3}\tau$ space, the distorted yield surface can be expressed as the set of yield points $(\sigma, \sqrt{3}\tau)$ which all satisfy the yield condition (1). For the uniaxial tensile pre-stress, the yield condition yields

$$f = \left[1 - c\,\frac{3\left(\frac{\sigma}{3} - \frac{\alpha_{11}}{2}\right)\alpha_{11}}{\sqrt{6\left(\frac{\sigma}{3} - \frac{\alpha_{11}}{2}\right)^2 + \frac{2}{3}(\sqrt{3}\tau)^2}}\right] \cdot \left[6\left(\frac{\sigma}{3} - \frac{\alpha_{11}}{2}\right)^2 + \frac{2}{3}(\sqrt{3}\tau)^2\right] - \frac{2}{3}k^2 = 0, \quad (22)$$

which is shown in Figure 5.

4. Identification of Parameters

The identification method is based on comparison of parametric descriptions of the stress-strain curve, and distorted yield surface in σ–$\sqrt{3}\tau$ space with experimental data. Significant features of curves generated by model, e.g., starting point, initial slope, limit value, width etc. are chosen. Proposed method uses 10 experimentally determined values $A_1, A_2, A_3, B_1, B_2, C_1, C_2, D_1, D_2, D_3$. The system of nonlinear equations, which includes known values $A_1, \ldots, D_3$ and unknown parameters $a_1, a_2, \kappa_1, \kappa_2, c, k_0$ is formulated, and the system is solved in the closed form.

In Figures 6, 7, 8, and 9, graphical interpretation of four experiments is depicted. The first experimental input, referred to as *the A experiment*, is the stress-strain diagram. Three parameters A_1, A_2 and A_3 comes from this experiment, see Figure 6. The second one, referred to as *the B experiment*, is the stress-strain diagram with reversion of loading at a certain level $\epsilon^{\mathrm{p}}_{11,B}$ of plastic strain. Two parameters B_1 and B_2 are stipulated by this experiment, see Figure 7. The third one, referred to as *the C experiment*, is the stress-strain diagram with reversion of loading at a different level $\epsilon^{\mathrm{p}}_{11,C}$ of plastic strain. Other two parameters, C_1 and C_2, are determined by this virtual experiment, see Figure 8. Finally, the fourth experiment referred as *the D experiment*, is done. Three parameters D_1, D_2, and D_3, are determined from experimentally detected distorted yield surface, see Figure 9. In sum, four experiments named A, B, C and D are necessary to obtain input data for identification method.

The stress-strain curve analytical model is given by Equation (21). Comparison of initial value

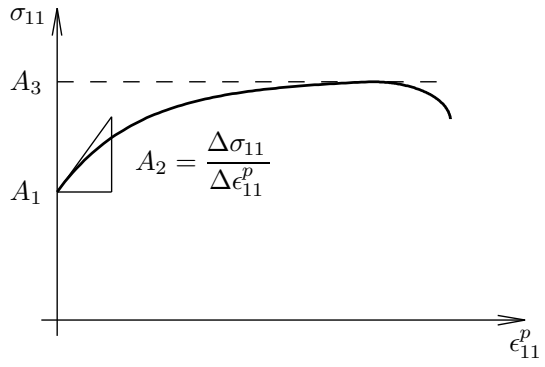

Figure 6: The A experiment, parameters A_1, A_2 and A_3.

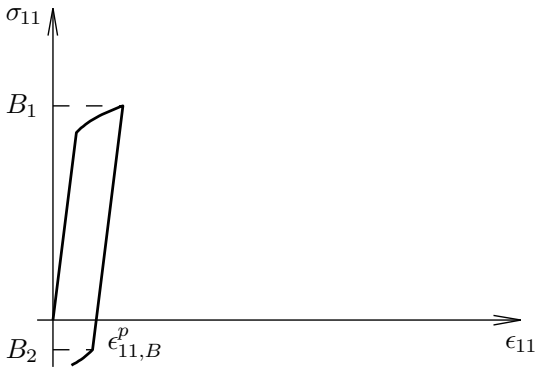

Figure 7: The B experiment, parameters B_1 and B_2.

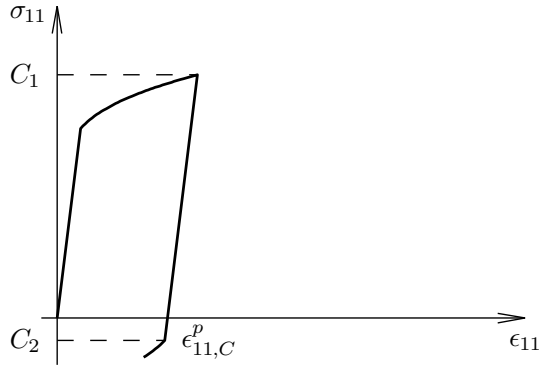

Figure 8: The C experiment, parameters C_1 and C_2.

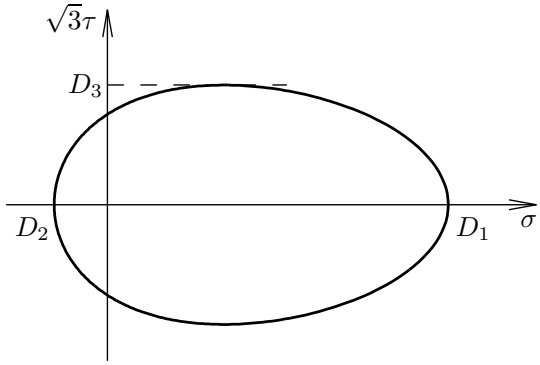

Figure 9: The D experiment, parameters D_1, D_2 and D_3.

of the stress-strain curve generated by model with experimentally determined one yields

$$A_1 = \sigma_{11}(\epsilon^{\mathrm{p}}_{11})\big|_{\epsilon^{\mathrm{p}}_{11}=0} = \sigma_Y = k_0. \tag{23}$$

Similarly, the initial slope can be expressed by

$$A_2 = \frac{\partial\sigma_{11}}{\partial\epsilon^{\mathrm{p}}_{11}}(\epsilon^{\mathrm{p}}_{11})\big|_{\epsilon^{\mathrm{p}}_{11}=0} = \frac{1}{2}\kappa_1(1-\kappa_2 k_0) + \frac{1}{2}\sqrt{\frac{3}{2}}k_0 a_1 c + \frac{3}{2}a_1, \tag{24}$$

and limit value of the stress-strain curve

$$A_3 = \lim_{\epsilon^{\mathrm{p}}_{11}\to+\infty}\sigma_{11}(\epsilon^{\mathrm{p}}_{11}) = \frac{1}{\kappa_2}\frac{1}{\sqrt{1-\dfrac{c}{a_2}}} + \sqrt{\frac{3}{2}}\frac{1}{a_2}. \tag{25}$$

From Equation (21), comparison of the yield stress in tensile direction ($\oplus$) at a certain $(\epsilon^{\mathrm{p}}_{11,B})$ level of plastic deformation with an experimental value yields

$$B_1 = \sigma_{11}(\epsilon^{\mathrm{p}}_{11,B})^{\oplus} = \frac{k(\epsilon^{\mathrm{p}}_{11,B})}{\sqrt{1-\alpha_{11}(\epsilon^{\mathrm{p}}_{11,B})c\sqrt{\dfrac{3}{2}}}} + \frac{3}{2}\alpha_{11}(\epsilon^{\mathrm{p}}_{11,B}). \tag{26}$$

Similarly, the yield stress in the opposite direction ($\ominus$) at the same ($\epsilon^{\mathrm{p}}_{11,B}$) level of plastic deformation yields

$$B_2 = \sigma_{11}(\epsilon^{\mathrm{p}}_{11,B})^{\ominus} = -\frac{k(\epsilon^{\mathrm{p}}_{11,B})}{\sqrt{1+\alpha_{11}(\epsilon^{\mathrm{p}}_{11,B})c\sqrt{\frac{3}{2}}}} + \frac{3}{2}\alpha_{11}(\epsilon^{\mathrm{p}}_{11,B}). \tag{27}$$

Following parametric expressions for the C experiment are the same as in the case of B experiment

$$C_1 = \sigma_{11}(\epsilon^{\mathrm{p}}_{11,C})^{\oplus} = \frac{k(\epsilon^{\mathrm{p}}_{11,C})}{\sqrt{1-\alpha_{11}(\epsilon^{\mathrm{p}}_{11,C})c\sqrt{\frac{3}{2}}}} + \frac{3}{2}\alpha_{11}(\epsilon^{\mathrm{p}}_{11,C}), \tag{28}$$

$$C_2 = \sigma_{11}(\epsilon^{\mathrm{p}}_{11,C})^{\ominus} = -\frac{k(\epsilon^{\mathrm{p}}_{11,C})}{\sqrt{1+\alpha_{11}(\epsilon^{\mathrm{p}}_{11,C})c\sqrt{\frac{3}{2}}}} + \frac{3}{2}\alpha_{11}(\epsilon^{\mathrm{p}}_{11,C}). \tag{29}$$

Regarding the parametric description of the D experiment, the distorted yield surface in σ–$\sqrt{3}\tau$ space is shown in Figure 9. As significant points, the left, the right, and the upper peak are chosen. This distorted surface is determined by Equation (22). The analysis of Equation (22) implies that the left and the right peak of the distorted yield surface in σ–$\sqrt{3}\tau$ space may be expressed as

$$D_1 = \frac{k(\epsilon^{\mathrm{p}}_{11,D})}{\sqrt{1-\alpha_{11}(\epsilon^{\mathrm{p}}_{11,D})c\sqrt{\frac{3}{2}}}} + \frac{3}{2}\alpha_{11}(\epsilon^{\mathrm{p}}_{11,D}) \tag{30}$$

and

$$D_2 = -\frac{k(\epsilon^{\mathrm{p}}_{11,D})}{\sqrt{1+\alpha_{11}(\epsilon^{\mathrm{p}}_{11,D})c\sqrt{\frac{3}{2}}}} + \frac{3}{2}\alpha_{11}(\epsilon^{\mathrm{p}}_{11,D}). \tag{31}$$

This expression is possible if one declares $\sqrt{3}\tau = 0$ in Equation (22). Consequently, the upper peak can be defined as a maximum of implicit function f from Equation (22). Using theorem related to the implicit function (derivation of implicit function), one may obtain the upper peak value

$$D_3 = \sqrt{2}\,k(\epsilon^{\mathrm{p}}_{11,D})\frac{\sqrt{1-\sqrt{1-\frac{3}{2}\alpha^2_{11}(\epsilon^{\mathrm{p}}_{11,D})\,c^2}}}{\sqrt{\frac{3}{2}}\,\alpha_{11}(\epsilon^{\mathrm{p}}_{11,D})\,c}. \tag{32}$$

The calibration procedure may be summarized as follows.

First, the k_0 parameter obeys Equation (23) stated in *the A experiment* subsection. One can write

$$k_0 = A_1. \tag{33}$$

Second, the c parameter obeys Equations (30), (31), and (32) stated in *the D experiment*. This system can be solved analytically. The solution for the c variable is

$$c = \frac{3 \cdot \sqrt{(D_1 - D_2)(D_1 - D_2 - 2D_3)}}{(D_1 - D_2 - D_3)\left[D_1 + D_2 - \sqrt{(D_1 - D_2)(D_1 - D_2 - 2D_3)}\right]}. \tag{34}$$

Third, to evaluate the a_2 parameter, two values of backstress, $\alpha_{11}(\epsilon^{\mathrm{p}}_{11,B})$ and $\alpha_{11}(\epsilon^{\mathrm{p}}_{11,C})$, flow from Equations (26), (27), (28), and Equation (29). The system (26), (27) forms the cubic equation

$$A\alpha^3_{11,B} + B\alpha^2_{11,B} + C\alpha_{11,B} + D = 0, \tag{35}$$

which

$$A = \frac{9}{2}\sqrt{\frac{3}{2}}c\,, \qquad B = -3\sqrt{\frac{3}{2}}c(B_1 + B_2)\,, \tag{36}$$

$$C = \sqrt{\frac{3}{2}}c(B_1^2 + B_2^2) + 3(B_1 - B_2)\,, \quad D = -(B_1^2 - B_2^2)\,, \tag{37}$$

where the discriminant may be rewritten as

$$\Delta = 18ABCD - 4B^3D + B^2C^2 - 4AC^3 - 27A^2D^2. \tag{38}$$

It can be easily shown that for $B_2 < 0$, i.e., if the plastic deformation in the reversed direction occurs in the compressive state, not in tensile one, $\Delta < 0$ and this equation has the only one real solution (root). Moreover, this solution can be expressed as

$$\begin{aligned}\alpha_{11,B} = &-\frac{B}{3A} \\ &- \frac{1}{3A}\sqrt[3]{\frac{1}{2}\left[2B^3 - 9ABC + 27A^2D + \sqrt{-27A^2\Delta}\right]} \\ &- \frac{1}{3A}\sqrt[3]{\frac{1}{2}\left[2B^3 - 9ABC + 27A^2D - \sqrt{-27A^2\Delta}\right]},\end{aligned} \tag{39}$$

and similarly for the term $\alpha_{11,C}$. At this moment, Equation (18) with the initial condition $\alpha_{11,0} = 0$ can be rewritten as

$$a_1 = -\sqrt{\frac{2}{3}}\frac{1}{a_2\epsilon^{\mathrm{p}}_{11,B}}\ln\left(1 - \sqrt{\frac{3}{2}}\alpha_{11,B}a_2\right) \tag{40}$$

for the $\epsilon^{\mathrm{p}}_{11,B}$ level of reversion and

$$a_1 = -\sqrt{\frac{2}{3}}\frac{1}{a_2\epsilon^{\mathrm{p}}_{11,C}}\ln\left(1 - \sqrt{\frac{3}{2}}\alpha_{11,C}a_2\right). \tag{41}$$

for the $\epsilon^{\mathrm{p}}_{11,C}$ level of reversion. After some algebra, two equations yield

$$\left(1 - \sqrt{\frac{3}{2}}\alpha_{11,B}a_2\right)^{\epsilon^{\mathrm{p}}_{11,C}/\epsilon^{\mathrm{p}}_{11,B}} + \sqrt{\frac{3}{2}}\alpha_{11,C}a_2 - 1 = 0. \tag{42}$$

If the $\epsilon^{\mathrm{p}}_{11,C}/\epsilon^{\mathrm{p}}_{11,B}$ term equals 2, the previous relation forms a quadratic equation and its solution is

$$a_2 = \sqrt{\frac{2}{3}}\,\frac{2\alpha_{11,B} - \alpha_{11,C}}{\alpha^2_{11,B}}. \tag{43}$$

This of course brings some restriction to the experiment.

Four, the a_1 parameter flows from Equation (40).

Five, the κ_2 parameter flows from Equation (25), which may be expressed by

$$\kappa_2 = \frac{1}{\sqrt{1 - \dfrac{c}{a_2}} \cdot \left(A_3 - \sqrt{\dfrac{3}{2}}\dfrac{1}{a_2} \right)}. \tag{44}$$

Finally, κ_1 parameter flows from Equation (24), which may be expressed as

$$\kappa_1 = \frac{2A_2 - \sqrt{\dfrac{3}{2}}k_0 a_1 c - 3a_1}{1 - \kappa_2 k_0}. \tag{45}$$

5. Verification of Identification Method

In this section, usage of the identification method is demonstrated. Since no complex experimental data are available, virtual experimental data are used as inputs.

c	0.009	MPa^{-1}
a_1	4 000	MPa
a_2	0.01	MPa^{-1}
κ_1	10 000	MPa
κ_2	0.004	MPa^{-1}
k_0	400	MPa

Table 1: *set up parameters*

c	0.0114	MPa^{-1}
a_1	3 504	MPa
a_2	0.0122	MPa^{-1}
κ_1	8 701	MPa
κ_2	0.0046	MPa^{-1}
k_0	412	MPa

Table 2: *identified parameters*

c	27 %
a_1	14 %
a_2	13 %
κ_1	13 %
κ_2	15 %
k_0	3 %

Table 3: *error of identification*

First, a set of artificial material parameters was chosen, see Table 1. Note that for specified parameters, thermodynamic & convexity condition expressed by Inequality (12) is fulfilled. Scripts for numerical simulation of requested experiments, i.e., experiment A, B, C and D, were coded in Matlab. These virtual experiments were performed and interpreted graphically. Based on these graphs, parameters $A_1, \ldots, D_3$ were read and used to identify the model's parameters. The identified parameters are shown in Table 2, error of identification can be seen in Table 3. Moreover, comparison of model's behavior for 'set up' and 'identified' material parameters in terms of stress-strain curve and distorted yield surface is plotted in Figure 10 and Figure 11, respectively.

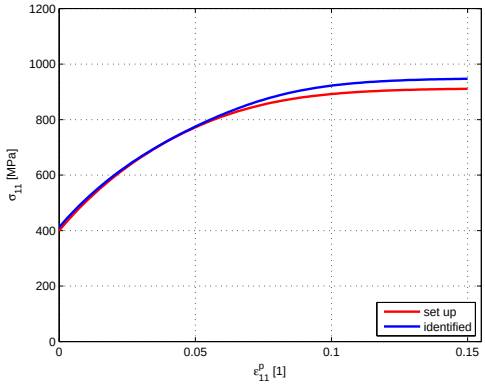

Figure 10: Comparison of set up and identified stress-strain curve.

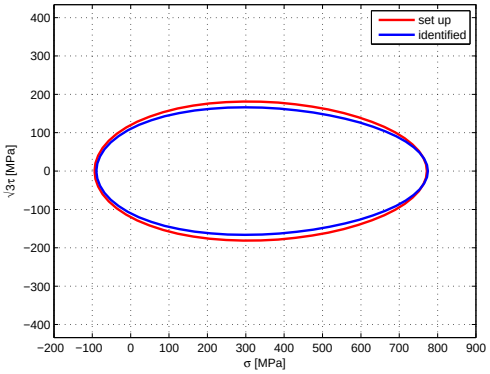

Figure 11: Comparison of set up and identified distorted yield surface.

6. Conclusions

Modern experiments show that plastic deformation of many metals causes anisotropy in plastic behavior. This anisotropy is manifested by distortion of the yield surface in the direction of load. In order to supply phenomenological description this effect, Feigenbaum and Dafalias (2007) proposed model based on the fourth order anisotropic tensor. This model is complemented by three simplified versions, where the simplest one is referred to as *the α-model with constant distortional parameter*. This model includes set of six material parameters k_0, a_1, a_2, κ_1, κ_2 and c that must be identified from experimental data.

The identification method proposed in this paper is based on the comparison of experimentally obtained stress-strain curves and a distorted yield surface curve in σ–$\sqrt{3}\tau$ space with analytical formulas of these curves. In sum, four experiments are necessary to be performed. Each of the discussed curves has significant features, e.g., start point, initial slope, width, extreme, which can be expressed analytically using model's parameters. Thus, ten experimentally determined parameters $A_1, A_2, A_3, B_1, B_2, C_1, C_2, D_1, D_2$, and D_3 are used for compilation of the system of ten nonlinear equations for six unknown parameters k_0, a_1, a_2, κ_1, κ_2, and c. This system can be solved in a closed-form, i.e. explicit expressions for each of unknown parameters.

Identification method was tested. Due to the absence of complex experimental data, virtual experiments are done. At first, a set of admissible parameters is proposed. Based on these parameters, numerical calculations in Matlab software were done. Using these virtual experimental data, the identification procedure was performed.

The proposed identification method seems to be applicable. Although maximum error in determination of parameters reached almost $30\,\%$, see Table 3, the error does not cause a large deviation of either stress-strain curves of distorted yield surfaces. These errors may be caused by the nonlinear behavior of the model, and they are related to its sensitivity.

ACKNOWLEDGEMENTS

This paper was supported by the Grant Agency of the Czech Republic, Project No. 101/09/1630.

7. References

Feigenbaum, H.P., Dafalias, Y.F. (2007). Directional distortional hardening in metal plasticity within thermodynamics. *Int.J. Solids Struct.*, 44, 7526–7542.

Feigenbaum, H.P. *Directional Distortional Hardening in Plasticity Based on Thermodynamics.* Davis: University of California, 2008. [dissertation].

Feigenbaum, H.P., Dafalias, Y.F. (2008). Simple model for directional distortional hardening in metal plasticity within thermodynamics. *J. Eng. Mech.*, 134, 730–738.

François, M. (2001). A plasticity model with yield surface distortion for non proportional loading. *Int. J. Plast.*, 17, 703–717.

Ortiz, M., Popov, E.P. (1983). Distortional hardening rules for metal plasticity. *J. Eng. Mech.*, 109, 1042–1057.

Plešek, J., Křístek, A. (1997). Assessments of methods for locating the point of initial yield. *Comp. Meths. Appl. Mech. Engng.*, 141, 389-397.

Plešek, J., Feigenbaum, H.P., Dafalias. Y.F. (2010). Convexity of yield surface with directional distortional hardening rules. *J. Eng. Mech.*, 136, 477–484.

Wu, H.C.; Yeh, W. (1991). On the experimental determination of yield and some results of annealed 304 stainless steel. *Int. J. Plast.*, 7, 803–826.